Plant, Cell & Environment

Plant, Cell and Environment (2015) **38**, 2735–2746 doi: 10.1111/pce.12584

Original Article

Leaf hydraulic conductance varies with vein anatomy across *Arabidopsis thaliana* wild-type and leaf vein mutants

Marissa A. Caringella[1], Franca J. Bongers[1,2,3] & Lawren Sack[1]

[1]*Department of Ecology and Evolutionary Biology, University of California, Los Angeles, CA 90095, USA,* [2]*Plant Ecophysiology, Institute for Environmental Biology, Utrecht University, 3584 CH Utrecht, The Netherlands and* [3]*Centre for Crop Systems Analysis, Wageningen University, 6708 PB Wageningen, The Netherlands*

ABSTRACT

Leaf venation is diverse across plant species and has practical applications from paleobotany to modern agriculture. However, the impact of vein traits on plant performance has not yet been tested in a model system such as *Arabidopsis thaliana*. Previous studies analysed cotyledons of *A. thaliana* vein mutants and identified visible differences in their vein systems from the wild type (WT). We measured leaf hydraulic conductance (K_{leaf}), vein traits, and xylem and mesophyll anatomy for *A. thaliana* WT (Col-0) and four vein mutants (*dot3-111* and *dot3-134*, and *cvp1-3* and *cvp2-1*). Mutant true leaves did not possess the qualitative venation anomalies previously shown in the cotyledons, but varied quantitatively in vein traits and leaf anatomy across genotypes. The WT had significantly higher mean K_{leaf}. Across all genotypes, there was a strong correlation of K_{leaf} with traits related to hydraulic conductance across the bundle sheath, as influenced by the number and radial diameter of bundle sheath cells and vein length per area. These findings support the hypothesis that vein traits influence K_{leaf}, indicating the usefulness of this mutant system for testing theory that was primarily established comparatively across species, and supports a strong role for the bundle sheath in influencing K_{leaf}.

Key-words: bundle sheath; leaf anatomy; leaf hydraulics; vein density; VLA.

INTRODUCTION

Across terrestrial ecosystems, leaves are diverse in size, structure and function. In particular, the leaf vein network is extremely variable across species, and angiosperms display the most diverse set of vein structures and systems (Ellis *et al.* 2009; Sack & Scoffoni 2013). Much of this diversity is linked to hydraulic design, as the leaf is a key component of the plant hydraulic system, which plays an important role in determining the maximum rate of photosynthetic gas exchange and growth (Tyree & Zimmermann 2002; Sack & Holbrook 2006; Brodribb *et al.* 2007). Leaf hydraulic conductance (K_{leaf}) provides a measure of how efficiently water is transported through the leaf, but important questions remain about the complex pathways that water follows to sites of evaporation (Buckley 2014; Rockwell *et al.* 2014). This is especially true regarding dynamic pathways outside the xylem, where water moves across the bundle sheath (BS) and mesophyll tissue to stomata. Therefore, in addition to the xylem conduits, leaf venation architecture and mesophyll structure and cellular anatomy are integral components in the leaf hydraulic pathway. We studied leaf vein mutants of the model species *Arabidopsis thaliana* to test the hypotheses for the anatomical determinants of leaf hydraulic conductance.

A number of studies conducted across a broad range of terrestrial plants have shown the importance of leaf hydraulic conductance (K_{leaf}), that is, the efficiency of water transport through the leaf, and indicated possible determinants of K_{leaf}. Thus, across diverse species, the maximum photosynthetic rate (A_{max}) and stomatal conductance (g_s) was positively correlated with K_{leaf} (Brodribb *et al.* 2007). Further, across diverse species, both A_{max}, g_s and K_{leaf} are often positively correlated with vein traits, including vein length per leaf area (VLA or 'vein density'; Sack & Frole 2006; Brodribb *et al.* 2007; Boyce *et al.* 2008; Brodribb *et al.* 2010; Sack & Scoffoni 2013). Additionally, greater xylem conduit numbers and diameters, high major VLA, more free-ending veins (FEVs) per unit area, BS anatomical traits and potentially the total area of mesophyll cells per leaf area (A_{mes}/A) may be positively correlated with higher K_{leaf} (Brodribb *et al.* 2007; McKown *et al.* 2010; Chatelet *et al.* 2013; Griffiths *et al.* 2013; Sack & Scoffoni 2013). However, while these correlations observed among K_{leaf} and vein traits that have been established across diverse species have also been supported by computer or physical simulations (Noblin *et al.* 2008; McKown *et al.* 2010), they have just begun to be tested across genotypes within given species. Such tests have the potential to establish a stronger causality, given the assumption of a similar background of other traits. Two very recent studies focused on 4 genotypes of *Coffea arabica* (Nardini *et al.* 2014) and 11 cultivars of *Oryza* (Xiong *et al.* 2014), and both confirmed the relationship of K_{leaf} to g_s and A_{max} but did not find a positive correlation of K_{leaf} with VLA. To our knowledge, there have been no previous studies of the hydraulic properties of wild-type (WT) and leaf vein mutant genotypes of *A. thaliana*, which provide a premier platform for testing the hypotheses for trait linkages.

Correspondence: L. Sack. e-mail: lawrensack@ucla.edu

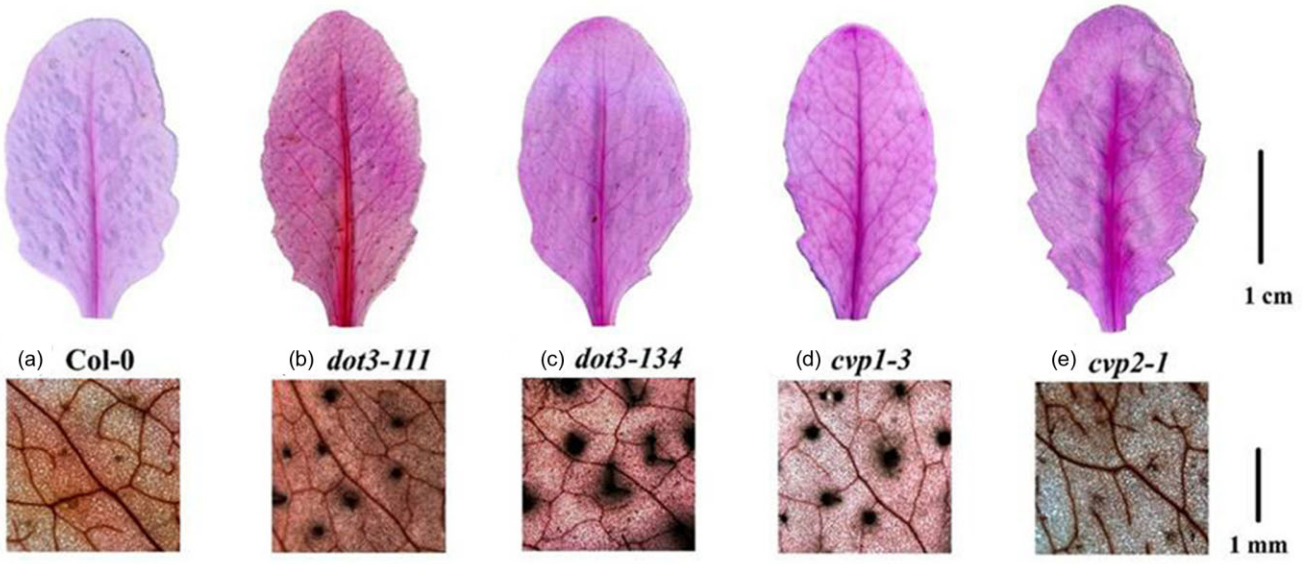

Figure 1. Whole cleared leaves and microscope images of cleared leaves (5×, dark spots are trichomes) for *Arabidopsis thaliana* genotypes (a) wild-type Col-0, (b) *dot3-111*, (c) *dot3-134*, (d) *cvp1-3* and (e) *cvp2-1*. Whole cleared leaves show that mature leaves of mutant genotypes did not retain traits seen in cotyledon classes. Microscopic images display the network of 3° and minor veins branching from a central 2° vein.

Knowledge about the molecular and developmental basis of leaf vein development has increased greatly by focusing on model species *A. thaliana* (Carland & Nelson 2004; Kang & Dengler 2004; Sieburth & Deyholos 2006; Petricka *et al*. 2008). As for typical angiosperm leaves, in *A. thaliana*, the venation system is constructed in a hierarchy, with the first three orders known as 'major veins'. In general, one or more first-order (1°) veins enter the lamina from the petiole, multiple secondary (2°) veins branch off along the length of the 1° vein(s), and third (3°) and higher order veins (known as 'minor veins') form a mesh throughout the lamina (Ellis *et al*. 2009). WT *A. thaliana* leaves have a central mid-vein with pairs of smaller high-arching secondary veins, forming closed loops nearly reaching the margins (known as 'brochidodromous' venation; Fig. 1a), enclosing a network of smaller tertiary and higher order veins (Kang & Dengler 2004). The development of leaf vein mutants with extreme phenotypes compared with the WT (Candela *et al*. 1999; Carland *et al*. 1999, 2002; Turner & Sieburth 2003; Carland & Nelson 2004; Clay & Nelson 2005; Sieburth & Deyholos 2006; Petricka *et al*. 2008; Robles *et al*. 2010) presents exciting possibilities for *A. thaliana* as a model system for leaf hydraulics. A recent study found variation among *A. thaliana* genotypes in stem hydraulic conductance and anatomy (Tixier *et al*. 2013). Here, we link K_{leaf} to vein traits and comprehensive mesophyll and xylem cellular anatomy in the true leaves of *A. thaliana* WT and four vein mutants.

Among vein mutants, six classes have been described (Petricka *et al*. 2008); here, we focus on two mutants from the parallel class (*defectively organized tributaries*, *dot3*) and two mutants from the open network class (*cotyledon vascular pattern*, *cvp*; Table 1). Cotyledons and juvenile leaves of parallel class mutants have more monocot-like parallel venation (Petricka *et al*. 2008), while open network class mutants have unclosed 2° veins and vascular islands (Carland *et al*. 1999; see Table 1 for the previously documented cotyledon/juvenile leaf vein traits). We focused on higher node (adult) leaves to determine if mutant phenotypes of cotyledons and juvenile leaves were retained and to analyse linkage with hydraulic function.

We tested the hypotheses for the relationships among venation architecture, hydraulic performance and anatomical structure among *A. thaliana* WT and mutants. We expected that (1) adult mutant leaves would display significant quantitative differences in venation traits from the WT, and the two mutant types (*dot* and *cvp*) and venation classes (parallel and open network) would differ. (2) Given that the WT has a vein system optimized during evolution, whereas mutant cotyledons/juvenile leaves have abnormal phenotypes, the WT would have higher K_{leaf} than the mutants. Indeed, previous studies of *A. thaliana* stomatal density and patterning mutants found reduced carbon assimilation and other morphological abnormalities due to direct and/or pleiotropic effects that cause measureable changes outside the targeted trait (Dow *et al*. 2014; Lawson *et al*. 2014). Most importantly, (3) we hypothesized based upon the previous studies conducted across species that shifts in specific vein and anatomical traits would be associated with shifts in K_{leaf} across *A. thaliana* genotypes (hypotheses listed in Table 2).

METHODS

Plant material and growth conditions

A. thaliana WT Col-0 (ecotype Columbia) and four venation mutants were studied. The mutants were selected based upon the previously documented variation in venation traits,

Table 1. *Arabidopsis thaliana* genotypes tested, mutant type, mutant cotyledon venation class, associated class traits (not found in mature leaves) and previous studies documenting cotyledon and juvenile leaf venation traits

Genotype	Mutant type	Venation class (cotyledon)	Venation class traits (cotyledon/juvenile leaf)	Reference
Col-0	WT Ecotype Columbia	WT	WT	Carland *et al.* 1999, 2002
dot3-111 *dot3-134*	*defectively organized tributaries* (*dot*)	Parallel	Monocot-like parallel venation More 2° veins exiting petiole Acute midrib to 2° branch angle Midrib same size as 2° veins	Petricka *et al.* 2008
cvp1-3 *cvp2-1*	*cotyledon vascular pattern* (*cvp*)	Open network	Unclosed 2° veins Disconnected 3° veins More FEV and vascular islands Fewer high order veins	Carland *et al.* 1999; Turner & Sieburth 2003; Carland & Nelson 2004

FEV, free-ending vein; WT, wild type.

including two mutants from two types and venation classes (Table 1); *defectively organized tributaries* mutants of the parallel class (*dot3-111* and *dot3-134*), and *cotyledon vascular pattern* mutants of the open network class (*cvp1-3* and *cvp2-1*). All mutants were originally generated from mutagenized M_2 seeds of the ecotype Columbia: *dot3-111* and *dot3-134* using diepoxybutane (Petricka *et al*. 2008), and *cvp1-3* and *cvp2-1* using methanesulfonate (Carland *et al*. 1999).

Seeds were sown on a 3:3:1:1 (peat moss, sandy loam, perlite, vermiculite) soil mix in a germination tray, kept in a dark chamber at 4 °C for 4 d to synchronize and optimize germination, and then grown in a greenhouse at 24 °C for 3 weeks. All plants were then transplanted to pots (d 3.8 cm, h 14 cm; Cone-tainer 610–09645; Li-Cor, Lincoln, NE, USA) and placed in a growth chamber at 22 °C and 70% relative humidity (RH) under a short-day light regime (9 h light, 15 h dark) with 200 μmol m^{-2} s^{-1} photosynthetically active radiation (after Wagner *et al*. 2011). Plants were watered daily and were 6–8 weeks old with ≥20 leaves before anatomical and hydraulic traits were assessed. We sampled fully mature, higher node (adult) leaves not yet showing signs of degradation (see Table 2 and Supporting Information Table S1 for measured traits).

Leaf hydraulic conductance

Leaf hydraulic conductance (K_{leaf}) was determined for 10 leaves collected from four individuals per mutant genotype, and 11 leaves for the WT. The evaporative flux method (EFM; Sack *et al*. 2002; Sack & Scoffoni 2012) was refined for small, delicate leaves. Pots were watered to full hydration the night before and morning of measurements. Leaves were cut from shoots with a fresh razor blade under ultrapure water (0.22 μm Thornton 200 CR; Millipore, Billerica, MA, USA); the petioles were wrapped in Parafilm to ensure a seal and then <1 mm was cut from the end underwater to ensure a fresh surface. The petiole was then rapidly connected under water to silicone tubing, which ran to a cylinder on a balance (±10 μg, models XS205 and AB265; Mettler Toledo, Columbus, OH, USA) connected to a computer which logged data in 30 s intervals and calculated steady-state transpirational flow rate through the leaf (E, mmol m^{-2} s^{-1}). The flow solution used was ultrapure water (0.22 μm Thornton 200 CR; Millipore) previously degassed under vacuum for >8 h using a vacuum pump (Model DOA-P704AA; Gast, Benton Harbor, MI, USA) and then re-filtered (0.2 μm, Syringe filter; Cole-Parmer, Vernon Hills, IL, USA).

The leaf attached to the tubing was placed abaxial side down in a wooden frame strung with fishing line (for support) above a box fan (Lakewood Engineering & Manufacturing Co., Chicago, IL, USA). Photosynthetically active radiation of >1000 μmol m^{-2} s^{-1} (LI-250 light meter; Li-Cor) was provided by floodlights (model 73828, 1000 W UV filter; Sears Roebuck, Hoffman Estates, IL, USA) suspended above the leaf surface, with a water-filled Pyrex container (Corning Inc., Corning, NY, USA) between leaves and light to absorb the heat. Leaf temperature was measured with a thermocouple (Cole-Parmer) and maintained at 23–28 °C (mean temperature was 24.6 ± 0.083 °C). Relative humidity (%RH) was monitored with a weather station (HOBO Micro Station with Smart Sensors; Onset, Bourne, MA, USA); mean %RH was 40.7 ± 0.49. To achieve a stable flow rate and allow the leaves to acclimate to high irradiance, leaves were allowed to transpire for at least 30 min or longer as necessary to achieve a coefficient of variation <0.05 for at least five measurements (Scoffoni *et al*. 2012). For all leaves, the mean time on the system was 45 ± 1.3 min, with a minimum of 30 min and a maximum of 75 min. Leaves were discarded if there was any sudden change in the flow rate. When flow rate stabilized, the average of the final 10 flow rate measurements was recorded, and leaf temperature was measured with the thermocouple. The leaf was then immediately removed from the tubing, any surface water removed from the petiole, and placed in a Whirl-Pak bag (Whirl-Pak, Nasco, Fort Atkinson, WI, USA) that had been exhaled in for humidity. A final water potential measurement was then made for each leaf.

Given that the fragile petioles of *A. thaliana* mutants were not well suited to the pressure chamber, we used an osmometer (Vapro, model 5520; Wescor, Logan, UT, USA) to measure the final water potential (Ψ_{leaf}). The sensitive thermocouple and electronic design of the osmometer enable a relatively short equilibration time of ~1 h (Ball & Oosterhuis

Table 2. Traits tested across *Arabidopsis* genotypes with symbols and units, followed by *a priori* hypotheses (H) for how each trait would affect K_{leaf} (i.e. as the trait increases in value will K_{leaf} increase ↑ or decrease ↓; based upon previous studies comparing diverse species: Aasamaa *et al*. 2001; Aasamaa *et al*. 2005; Brodribb *et al*. 2007; Sack & Scoffoni 2013; Krober *et al*. 2014), and significance in ANOVAs

				ANOVA 1	ANOVA 2 Differences among mutants	
Trait	Symbol	Units	H	All genotypes	Class	Genotype
Leaf hydraulics						
Leaf hydraulic conductance (leaf area basis)	K_{leaf}	mmol m^{-2} s^{-1} MPa^{-1}		*		*
Measurement leaf water potential (covariate)	Ψ_{leaf}	MPa		***	***	
Leaf venation architecture						
Total vein length per area	VLA	mm mm^{-2}	↑			
Major (1°, 2°, 3°) vein length per area	Major VLA	mm mm^{-2}	↑	*		
Primary vein length per area	1° VLA	mm mm^{-2}	↑			
Secondary vein length per area	2° VLA	mm mm^{-2}	↑	*		
Tertiary vein length per area	3° VLA	mm mm^{-2}	↑			*
Minor (4° and 5°) vein length per area	Minor VLA	mm mm^{-2}	↑			
Free-ending veins per area	FEV/A	# mm^{-2}	↑	**		
Midrib diameter	d_{midrib}	mm	↑			
Secondary vein diameter	d_2°	mm	↑			
Angle at which secondary branches off midrib		°	NA			
Total number of secondaries exiting the petiole		#	NA			
Gross leaf anatomy						
Leaf area	LA	cm^2	NA	***	*[a]	**
Leaf (lamina) thickness	LT	μm	↑			
Epidermal and mesophyll anatomy						
Upper cuticle thickness	$T_{cut, upper}$	μm	NA	*[a]	**	
Lower cuticle thickness	$T_{cut, lower}$	μm	NA	*[a]	**	
Upper epidermal thickness	$T_{epi, upper}$	μm	NA			
Lower epidermal thickness	$T_{epi, lower}$	μm	NA	*[a]	*[a]	
Spongy mesophyll tissue thickness	T_{spongy}	μm	↓			
Spongy mesophyll cell layers	SCL	#	↓	*		
Palisade mesophyll thickness	$T_{palisade}$	μm	↓[b]			
Palisade mesophyll cell layers	PCL	#	↓[b]	*		
Ratio palisade to spongy cell layers	PCL/SCL	units cancel	↑	*		
Upper epidermal cell cross-sectional area	$CA_{epi, upper}$	μm^2	NA			
Lower epidermal cell cross-sectional area	$CA_{epi, lower}$	μm^2	NA			
Spongy mesophyll cell cross-sectional area	CA_{spongy}	μm^2	NA			
Spongy mesophyll tissue percent airspace	Air_{spongy}	%	NA			
Palisade mesophyll cell cross-sectional area	$CA_{palisade}$	μm^2	NA			
Palisade mesophyll tissue percent airspace	$Air_{palisade}$	%	NA			
Total leaf lamina percent airspace	Air_{leaf}	%	NA			
Stomatal guard cell depth	GCD	μm	NA			
Bundle sheath extensions	BSE	Not present	NA			
Mean maximum vein-to-stomatal distance	D_m	μm	↓			
Spongy mesophyll surface area per leaf area	$A_{mes, sp}/A$	μm^2 μm^{-2}	↑	*		
Palisade mesophyll surface area per leaf area	$A_{mes, pal}/A$	μm^2 μm^{-2}	↑			
Bundle sheath cell surface area per leaf area	$A_{mes, bs}/A$	μm^2 μm^{-2}	↑			
Total mesophyll surface area per leaf area	A_{mes}/A	μm^2 μm^{-2}	↑			
Leaf vein cross-sectional anatomy						
Vascular bundle cross-sectional area	AC_{bundle}	μm^2	↑			
Number of bundle sheath cells (minor veins)	BSC	#	↑	*		**
Mean bundle sheath cell radial diameter (minor veins)	d_{bsc}	μm	↓			
Anatomical index of BS conductance (minor veins)	K_{bs}'	mm^{-2}	↑	*		*
Interveinal distance (minor veins)	IVD	μm	↓			
Vein-to-epidermal distance, upper	VED_{upper}	μm	↓[b]			
Vein-to-epidermal distance, lower	VED_{lower}	μm	↓			
Midrib number of xylem conduits	CN_{midrib}	#	↑	*		*
Midrib mean maximum conduit diameter	MCD_{midrib}	μm	↑			
Midrib mean conduit lumen area	LUA_{midrib}	μm^2	↑			
Minor vein number of xylem conduits	CN_{minor}	#	↑			*
Minor vein mean maximum conduit diameter	MCD_{minor}	μm	↑			
Minor vein mean conduit lumen area	LUA_{minor}	μm^2	↑			
Midrib theoretical leaf-specific conductivity	K_x', midrib	mmol m^{-1} s^{-1} MPa^{-1}	↑			
Minor vein theoretical leaf-specific conductivity	K_x', minor	mmol m^{-1} s^{-1} MPa^{-1}	↑			

ANOVA 1 tested trait variation across all five genotypes; ANOVA 2 tested trait variation across mutant genotypes nested within class. See Supporting Information Table S5 for complete ANOVA results (including n, F and P-values).

*$P < 0.05$; **$P < 0.01$; ***$P < 0.001$.

[a]Rendered not significant by false detection rate method (Benjamini & Hochberg 1995) applied to traits not hypothesized *a priori* to vary across genotypes differing in venation architecture (see the Methods section).

[b]Effect expected for amphistomatous leaves, as all five genotypes were.

2005). Published comparisons of pressure chamber and psychrometer water potential measurements found that with proper insulation and equilibration (both built-in to the Vapro osmometer), the two methods yield values that are tightly correlated, often with a nearly 1:1 relationship (Oosterhuis *et al*. 1983), although psychrometer values may be more negative at higher water potentials (Barigah *et al*. 2013). A leaf disc was removed with a cork borer and placed abaxial side up in the osmometer chamber within 10 s. The lamina disc was equilibrated for 40 min in the chamber, and 2–10 additional measurements were taken at 5–10 min intervals in *Auto Repeat* mode until the difference in values was <5%, for a minimum of 60 min total in the osmometer. We tested the seal of the osmometer using a solution of known osmolality that was left to equilibrate for 1 h in the same manner as the leaf discs for water potential measurements. In three tests of each of the two Vapro osmometers (six tests in total) using a 1000 mmol kg^{-1} solution, the mean measured value was 1004 ± 1.6 mmol kg^{-1} (this falls within the range of acceptable error for calibration of the Vapro osmometers, ±5 mmol kg^{-1}). The rest of the leaf was then rehydrated with the petiole under water, and leaf area was determined by scanning (flatbed scanner, Epson Perfection 4490) and analysing the image (ImageJ, NIH, Bethesda, MD, USA). K_{leaf} was calculated as $E/\Delta\Psi_{leaf}$, where $\Delta\Psi_{leaf} = -\Psi_{leaf}$ (because the water potential at the leaf petiole was ≈ 0), normalized by leaf area, and standardized to 25 °C to correct for changes in K_{leaf} caused by the temperature dependence of water viscosity (Weast 1974; Yang & Tyree 1993). We note that the leaves measured for K_{leaf} by the EFM are transpiring and thus partially dehydrated when steady-state flow is achieved; final leaf water potentials were observed in the range previously published for *Arabidopsis* leaves transpiring under high evaporative demand (Levin *et al*. 2007; Caldeira *et al*. 2014).

Leaf clearing and vein system analysis

We determined venation traits from one leaf from each of four individuals per genotype ($n = 4$ for each of the five genotypes). Leaves were cleared, stained, imaged and analysed according to standard protocols (Berlyn & Miksche 1976; Sack & Scoffoni 2012; Sack *et al*. 2012). Fully hydrated leaves were fixed in FAA (70% formalin–acetic acid–alcohol, 48% ethanol:10% formalin:5% glacial acetic acid:37% water), cleared in 5% sodium hydroxide and water, and stained with safranin and fast green. Cleared leaves were mounted with water in a transparent film (AF4300, 3M, St. Paul, MN, USA) and scanned (1200 dpi; flatbed scanner, Epson Perfection 4490, Long Beach, CA, USA) for quantification of leaf area and major vein lengths and diameters. Measurements of minor veins were made from images obtained using a light microscope (DMRB, Leica Microsystems, Buffalo Grove, IL, USA) with a 5× objective and digital camera (14. 2 Color Mosaic, Diagnostic Instruments, Sterling Heights, MI, USA) utilizing SPOT advanced imaging software (SPOT Imaging Solutions, Diagnostic Instruments). All images were manually analysed with ImageJ software (Version 1. 46r). We used sufficient magnification to ensure that all major veins were observed in the whole leaf scans (1.00 magnification, 47 pixels mm^{-1}) and multiple areoles were observed in the microscopic images of the minor veins (287× magnification, 813 pixels mm^{-1} in scale, resolving power: 1 pixel = 1.2 μm; Sack *et al*. 2014).

Major vein (1°, 2° and 3°) measurements were made for the entire leaf. We measured midrib (1°) projected area and length, and averaged three diameter measurements made in the middle of the top, center and bottom thirds of the midrib. We measured the branching angle of the 2° veins from the midrib for the two 2° veins on either side of the midrib closest to the center of the leaf. We also measured the number of vascular strands entering the lamina from the petiole (becoming 2° veins), the number of large 2° veins, the 2° vein length, the 3° vein length and the total major (1° + 2° + 3°) vein length per area (major VLA). From the microscopic images, we measured the diameters of the randomly selected 2° and 3° veins, the lengths of minor veins (4° and 5°) and the number of FEVs. Minor VLA and number of free-ending veins per leaf area (FEV/A) were calculated by dividing the minor vein length and the number of FEVs by the microscope image size corrected for the 2° vein area (area image – area 2° veins), and total VLA was calculated as the sum of the major and minor vein VLA. Given that minor VLA values might be affected by excluding major veins from the images, we confirmed that the results were robust by calculating leaf-scale values using a novel calculation that corrected for the area of the leaf taken up by major veins using the formula:

$$\text{Total VLA} = 1°\text{VLA} + 2°\text{VLA} + 3°\text{VLA} + \text{minor VLA} \times [1 - (1°\text{VPAA} + 2°\text{VPAA} + 3°\text{VPAA})], \quad (1)$$

where 1°, 2° and 3° VPAA are, respectively, the vein projected areas per leaf area of the first-, second- and third-order veins, determined as the product of their VLA and diameters. Values were very similar (for total VLA within 2–3%) using the two calculation methods; we present analyses in this paper based upon the values determined with the first method, the most commonly used in the literature (results of both methods are compared in Supporting Information Table S2).

Anatomical measurements

One leaf fixed in FAA from each of four individuals per genotype was sampled for cross-sectioning to determine leaf tissue, cell and cell wall dimensions (Oguchi *et al*. 2005; Tosens *et al*. 2012). A 1 × 0.5 cm rectangle was cut from the centre of each leaf, with the midrib centred lengthwise. Samples were slowly infiltrated with a mixture of ethanol and low-viscosity acrylic resin (L. R. White, London Resin Co., London, UK) under vacuum until completely infiltrated. Samples were placed in resin-filled gelatin capsules and allowed to set overnight in an oven at 55 °C. Embedded samples were then sectioned in the transverse plane with glass knives (LKB 7800 KnifeMaker; LKB Produkter,

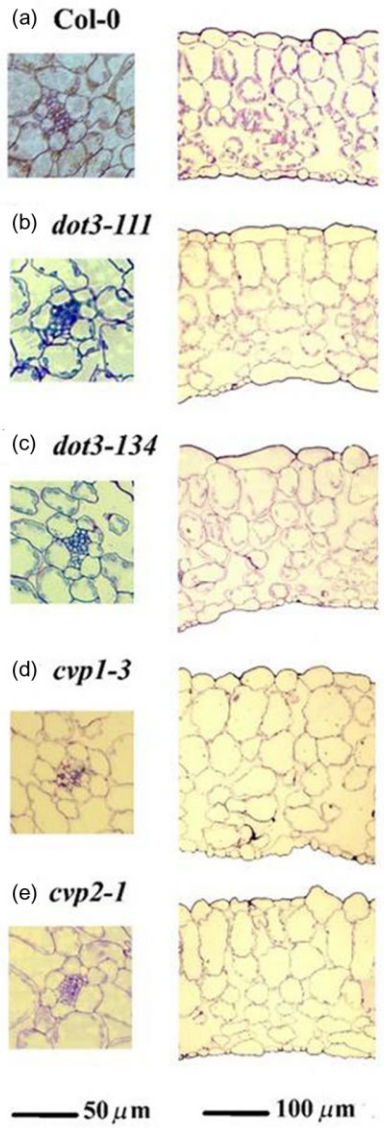

Figure 2. Microscopic images of leaf cross sections showing a minor vein with bundle sheath and entire lamina for *Arabidopsis thaliana* genotypes (a) wild-type Col-0, (b) *dot3-111*, (c) *dot3-134*, (d) *cvp1-3* and (e) *cvp2-1*. See Table 2 for significant differences in epidermal and mesophyll anatomy and leaf vein cross-sectional anatomy.

Bromma, Sweden) at 1 μm thickness using a rotary microtome (Leica Ultracut E, Reichert-Jung, Arcadia, CA, USA). Cross sections were stained on slides with 0.01% toluidine blue in 1% sodium borate and were imaged using the 20× and 40× objectives of a light microscope and camera (Leica DMRB; 14.2 Color Mosaic with SPOT advanced imaging software) and manually analysed with ImageJ.

To comprehensively phenotype the leaf cross-sectional anatomy (Fig. 2), we measured tissue thicknesses (whole lamina, spongy and palisade mesophyll, epidermis and cuticle), the cross-sectional areas, perimeters and diameters of cells (spongy, palisade, BS, epidermal pavement cells and guard cells), the cross-sectional areas and perimeters (outer and inner) of the minor veins, the interveinal distance (IVD), and the adaxial and abaxial minor vein-to-epidermal distances (from BS to epidermis; VED). For measurement of tissue and cell dimensions, the lamina image was divided into three sections and each trait was averaged from a measurement made near the centre of each of the three sections. Minor vein traits were averaged from two minor veins per individual; the radial diameters of the smallest, medium and largest cells per BS were measured and the means were averaged.

We calculated traits that would contribute to the conductance of water through the BS (see Fig. 2 for images of minor veins with BS). We expected that for a given BS cell membrane conductivity, the BS conductance would increase with the number of cells arranged around the perimeter of the BS (BSC), and decline with the radial diameter of the BS cells (d_{bsc}) given a greater distance for symplastic and apoplastic flow across the BS. We thus derived an anatomical index of minor vein BS conductance per area (K_{bs}'; mm^{-2}):

$$K_{bs}' = \mathrm{BSC}/d_{bsc} \times \text{Minor VLA}. \quad (2)$$

For the midrib and minor veins, all xylem conduits were measured; conduits were considered as ellipses, and lumen area was calculated using the major and minor axes. The theoretical conductivities (K_x'; mmol s^{-1} m MPa^{-1}) of the major and minor veins were calculated using the Hagen–Poiseuille equation modified forellipses (Lewis & Boose 1995; Cochard *et al*. 2004; Dettmann *et al*. 2013):

$$K_x' = \frac{J}{\Delta p} = \frac{V}{t \times \Delta p} = \frac{\pi(a^3 \times b^3)}{4\eta L(a^2 + b^2)}, \quad (3)$$

where J is the rate of volume flow, Δp is the pressure gradient along a shoot of length L, V is the volume of water, t is the time, η is the viscosity of water, a is the major axis and b is the minor axis. Conduit conductivities were calculated individually and summed for each vein. The resulting conductivities were normalized by leaf area to generate theoretical leaf-specific conductivity (K_x', mmol s^{-1} m^{-1} MPa^{-1}; Choat 2011).

Maximum vein-to-stomatal distance (D_m) has been described as an anatomical trait closely correlated with VLA, and which may correlate with or determine the conductance outside the xylem (Brodribb *et al*. 2007). The D_m was measured as the hypotenuse of a right triangle bound by the interveinal distance and vein-to-epidermal distance:

$$D_m = \sqrt{(\mathrm{IVD}/2)^2 + \mathrm{VED}^2}. \quad (4)$$

All genotypes were amphistomatous, so $D_{m,\,upper}$ and $D_{m,\,lower}$ were measured separately, and because the two epidermises represent flow pathways in parallel, the overall D_m was determined as the harmonic mean of $D_{m,\,upper}$ and $D_{m,\,lower}$ (i.e. the inverse of the mean of their inverses).

The surface area of the mesophyll cells per leaf area (A_{mes}/A) was calculated as a measure of the cell surface available for CO_2 absorption or water evaporation within the leaf (Nobel *et al*. 1975; Tosens *et al*. 2012). The A_{mes}/A was determined separately for spongy and palisade mesophyll tissue

layers (spongy and palisade cells modelled as spheres and capsules, respectively; Chatelet *et al*. 2013), and additionally, we included a novel correction to account for minor vein vascular bundles, considering half the bundle to occur in spongy and half in palisade tissue:

$$\frac{A_{mes}}{A} = SA_{cell} \times \frac{[T_{tissue} - (ASF_{tissue} \times T_{tissue}) - (0.5CSA_{bundle} \times VLA_{minor})]}{V_{cell}}, \quad (5)$$

where SA is the surface area, V is the volume, ASF is the airspace fraction, T is the thickness, CSA_{bundle} is the cross-sectional area of the vascular bundle and VLA_{minor} is the minor vein length per area. A_{mes}/A was then calculated for the BS:

$$\frac{A_{mes,bs}}{A} = P_{bs} \times VLA_{minor}, \quad (6)$$

where P_{bs} is the outer perimeter of the BS. The three tissues (spongy, palisade and BS) were then summed to achieve total A_{mes}/A.

Statistical analysis

We used two ANOVAs to test for the differences in measured traits among genotypes. Firstly, we tested for the differences across all five genotypes in each trait with a one-way ANOVA and, when significant, we applied Tukey's post-hoc tests to resolve the differences among the given genotypes. Secondly, to test for putative differences among mutant classes, we used an ANOVA with mutant genotype nested within mutant class (see Supporting Information Table S5 for n, F and P-values for the two ANOVAs). For all comparisons, mean K_{leaf} was also analysed, including steady-state leaf water potential (Ψ_{leaf}) as a cofactor, to account for K_{leaf} being dynamic with leaf water status (Blackman *et al*. 2009; Scoffoni *et al*. 2012).

Correlations were performed on raw and log-transformed data for measured traits across all genotypes (see Supporting Information Table S3 for correlation matrix, Pearson's r shown).

We focused on testing only previously hypothesized relationships and thus did not generally apply a correction for multiple correlation tests, as that would have reduced the power to test *a priori* hypotheses. We thus discuss as significant (1) those differences resolved by ANOVAs for traits hypothesized *a priori* to differ with venation architecture among genotypes, including vein traits and palisade and spongy mesophyll cell layers (Wylie 1939) and (2) the significant correlations of K_{leaf} with traits expected to be influential based upon the previous studies (see hypotheses in Table 2). However, we provided data on a wider set of phenotypic traits to fully characterize these mutants, and for readers interested in applying a multiple test correction for 'mining' for unhypothesized significant phenotypic differences from the ANOVA results (Table 2), we provided the significance level required by the false detection rate method to avoid the risk of inflated type I error (Benjamini & Hochberg 1995).

All analyses were performed in R version 3.0.1 (http://www.r-project.org/).

RESULTS

Variation in venation of true leaves among mutants and WT

The true leaves of the mutants did not show the qualitative phenotypes previously described for cotyledons. The true leaves of the parallel class mutants (*dot3-111* and *dot3-134*) did not have parallel venation, and we found no significant differences in 2° branching angle, number of 2° veins exiting the petiole or diameter of the midrib (d_{midrib}) between the WT and the *dot* mutants (Table 2 and Supporting Information Table S1). Similarly, the true leaves of the open network class mutants (*cvp1-3* and *cvp2-1*) did not differ from the WT in 3° or minor vein length per area (Figs 1 & 3; Table 2). The open network class mutants did not generally have distinctively higher FEV/A; the mutant *cvp*2-1 had the highest mean value, 1.59 mm^{-2}, while the other mutant of this class, *cvp*1-3, had the lowest value, 0.648 mm^{-2} (Fig. 4c; Table 2).

However, we found statistically significant quantitative variation in vein traits among the genotypes. There were 1.5-fold differences across genotypes in 2° VLA and major VLA, with lowest values for the WT ($P < 0.05$; Fig. 3; Table 2), 0.711 ± 0.0391 and 1.25 ± 0.0548 mm mm^{-2}, respectively, and highest values for *dot3-111*, 1.09 ± 0.0752 and 1.88 ± 0.136 mm mm^{-2}. Mutants varied by 1.6-fold in 3° VLA ($P < 0.05$; Fig 3; Table 2), with *dot3-111* again having the highest value, 0.667 ± 0.0794 mm mm^{-2}. There was a 2.5-fold difference across the genotypes in FEV/A ($P < 0.05$; Fig. 4c; Table 2). We found no significant differences in 1°, minor or total VLA.

Variation among *A. thaliana* vein mutants and WT in leaf hydraulic efficiency

Mean K_{leaf} varied by threefold across all *A. thaliana* genotypes. The mean K_{leaf} ± SE of the WT was

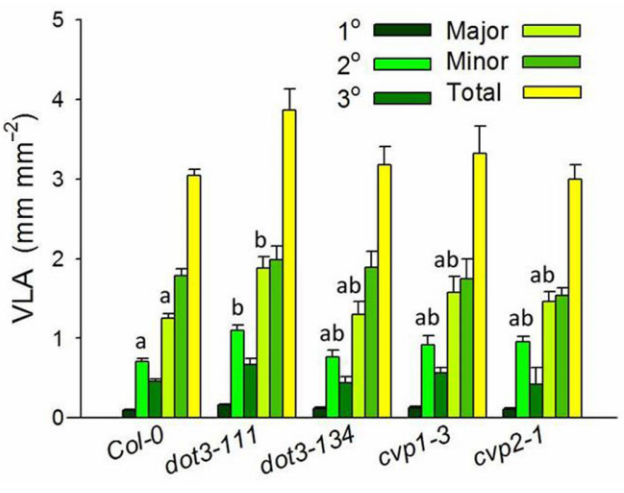

Figure 3. Mean vein length per area (VLA) ± SE for Col-0 (wild-type), *dot3-111*, *dot3-134*, *cvp1-3* and *cvp2-1*. There were significant differences in major VLA and 2° VLA among all five genotypes ($P < 0.05$; ANOVA 1). Differences (significant Tukey's test) indicated by different letters (a, b).

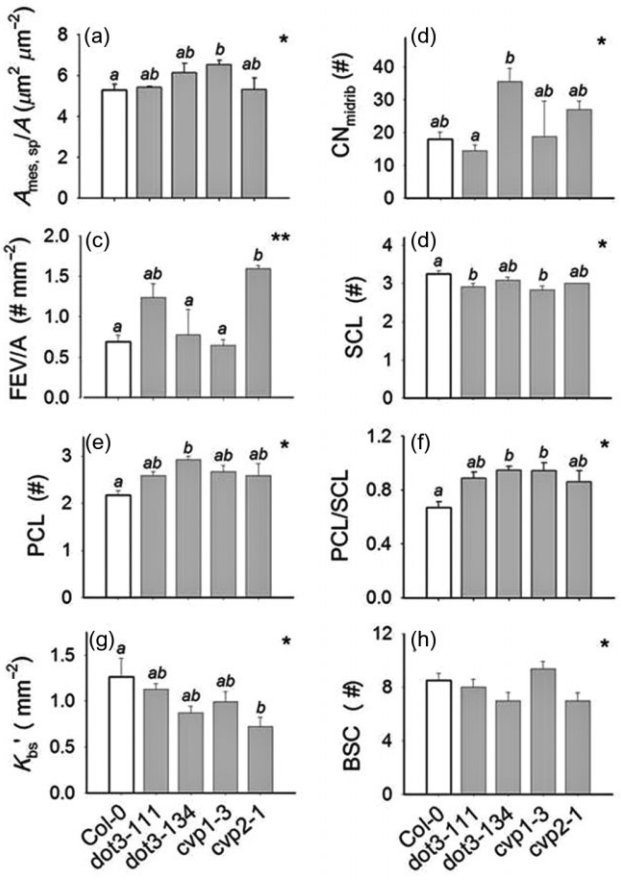

Figure 4. Bar plots of structural and anatomical traits (±SE) for Col-0 (wild-type), *dot3-111*, *dot3-134*, *cvp1-3* and *cvp2-1*: (a) area spongy mesophyll per leaf area, $A_{mes,\ sp}/A$; (b) number of xylem conduits in the midrib, CN_{midrib}; (c) number of free-ending veins per area, FEV/A; (d) number of spongy mesophyll cell layers, SCL; (e) number of palisade mesophyll cell layers, PCL; (f) ratio of palisade to spongy cell layers, PCL/SCL; (g) anatomical index of minor vein BS conductance per area, $K_{bs}' = BSC/d_{bsc} \times$ minor VLA; (h) number of BS cells (minor veins), BSC. Significant differences are shown for ANOVA 1 only (comparing all five genotypes) in the upper right hand corner of plots; $*P < 0.05$; $**P < 0.01$. Differences between genotypes (significant Tukey's test) are indicated by different letters (a, b).

4.36 ± 1.31 mmol m^{-2} s^{-1} MPa^{-1}, a value close to that reported in a previous study for the *A. thaliana* WT, 4 mmol m^{-2} s^{-1} MPa^{-1}, using the same Columbia ecotype and EFM method, although with a pressure chamber rather than the osmometer used here (Sade *et al.* 2014). The WT K_{leaf} values arose from a mean transpiration rate ± SE of 3.50 ± 0.739 mmol m^{-2} s^{-1} and a mean water potential driving force of -1.02 ± 0.0809 MPa. The mean K_{leaf} of the WT was significantly greater than that of the mutants, which varied from 1.43 ± 0.229 to 2.80 ± 0.579 mmol m^{-2} s^{-1} MPa^{-1} for *dot3-134* and *dot3-111*, respectively ($P < 0.001$; Tables 2 & 3). Final water potential values were similar across the genotypes; therefore, differences in K_{leaf} followed the same pattern as differences in transpiration (Supporting Information Table S4). Among the mutants, differences were significant among genotypes but not between venation classes, indicating more variation within *dot* and *cvp* mutant types than between the types ($P < 0.05$; Tables 2 & 3).

Differences in leaf gross structure, and mesophyll and vein anatomy

A. thaliana genotypes varied significantly in aspects of leaf structure and tissue organization, although they were very similar in many mesophyll anatomy traits. Individual leaf area differed by twofold among all genotypes ($P < 0.001$), with significant differences between *cvp* and *dot* mutant types ($P < 0.05$), and among all mutants ($P < 0.01$; Tables 2 & 3). There was a significant variation in the number of layers of spongy and palisade mesophyll cells (SCL and PCL), and in the ratio of PCL:SCL among all genotypes ($P < 0.05$; Fig. 4d–f; Table 2). Spongy mesophyll surface area per leaf area ($A_{mes,sp}/A$) differed among all genotypes ($P < 0.05$; Fig. 4a; Table 2). The number of conduits in the midrib (CN_{midrib}) varied by 2.4-fold among all genotypes and also among mutants ($P < 0.05$; Fig. 4b; Table 2); the number of conduits in the minor veins (CN_{minor}) varied by 1.6-fold among mutants ($P < 0.05$; Table 2). Across all genotypes, there were significant differences in the number of minor vein BS cells (BSC) and minor vein BS conductance per area (K_{bs}'; $P < 0.05$: Fig. 4g,h; Table 2).

Correlation of mesophyll and bundle sheath traits with leaf hydraulic conductance

The higher K_{leaf} of the WT was not related to several vein traits that had been hypothesized to be influential based upon comparisons made across diverse species, including VLA, d_{bsc} and BSC (see the Introduction section; Supporting Information Table S3; Fig. 5a–c). However, across all

Table 3. Leaf morphological traits (mean ± SE) and hydraulic conductance for true leaves of the WT (Col-0) and four venation mutants: leaf area (LA), lamina thickness (LT), total surface area of mesophyll cells per leaf area (A_{mes}/A), total vein length per area (VLA) and leaf hydraulic conductance (K_{leaf})

Genotype	LA (cm^2)	LT (μm)	A_{mes}/A (mm^2 mm^{-2})	VLA (mm mm^{-2})	K_{leaf} (mmol m^{-2} s^{-1} MPa^{-1})
Col-0	2.48 ± 0.271	216 ± 13.5	15.8 ± 0.366	3.04 ± 0.0800	4.36 ± 1.31
dot3-111	1.91 ± 0.202	233 ± 12.9	18.6 ± 1.66	3.87 ± 0.266	2.80 ± 0.579
dot3-134	3.52 ± 0.270	219 ± 8.92	18.6 ± 0.723	3.18 ± 0.222	1.43 ± 0.229
cvp1-3	3.00 ± 0.252	234 ± 15.8	18.3 ± 0.496	3.32 ± 0.343	2.60 ± 0.587
cvp2-1	3.57 ± 0.303	233 ± 6.80	16.7 ± 0.426	3.00 ± 0.184	1.62 ± 0.244

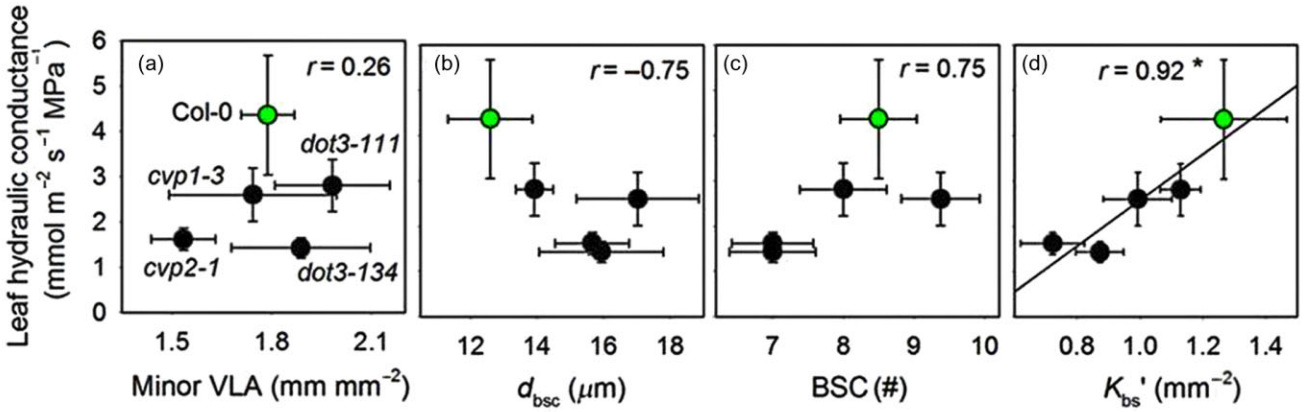

Figure 5. Correlations between K_{leaf} and (a) minor vein length per area (VLA), (b) d_{bsc} and (c) BSC, to illustrate how each component contributes to the anatomical index of minor vein bundle sheath conductance per area, K_{bs}' (d). Pearson's r shown (Supporting Information Table S3); $*P < 0.05$.

genotypes, we found a strong correlation of K_{leaf} with the anatomical index of minor vein BS conductance per area (K_{bs}' = BSC/d_{bsc} × Minor VLA; $r = 0.92$, $P < 0.05$; Fig. 5d).

DISCUSSION

The true leaves of the *A. thaliana* vein mutants studied did not reflect the differences previously documented for the cotyledon or juvenile leaves. However, we found a strong, novel variation in leaf hydraulic function and quantitative differences in anatomy and venation. Strong correlations between K_{leaf} and the anatomy of the path of water through the BS point to this tissue as an important locus for the determination of leaf hydraulic efficiency.

True leaves of mutants did not retain distinct phenotypes associated with venation class

The true leaves of *A. thaliana* did not retain the extreme phenotypes previously documented in cotyledons and juvenile leaves of the vein mutants. Contrary to hypothesis (1), the class distinctions documented for these mutants did not apply to mature leaves, and in general, the variation in hydraulic performance and xylem and mesophyll anatomy was not greater between than within mutant classes. Studies for over a decade into *A. thaliana* leaf and vein network development have shown that vein pattern depends upon gene expression and signal transduction pathways that can be altered (Scarpella *et al.* 2004). Thus, differential vein patterning, including the formation of free vein endings or interconnected veins, arises through alteration in the initiation of preprocambial branches and the timing of their development into veins before mesophyll differentiation. Most models attribute mutational defects to interruptions in patterns of auxin transport during organ development (Sachs 1975; Aloni 2001). Our findings of strong differences in venation between cotyledons (as previously described) and true leaves suggest that either differential gene expression affects vein development in the leaves of different ontogenetic stages or that plasticity of the developmental system could cover up defects in the true leaves.

Extra-xylary traits contribute to significantly higher leaf hydraulic conductance in WT

The WT had substantially higher K_{leaf} than the vein mutants (Table 3; Fig. 5), which supported hypothesis (2). The higher K_{leaf} of the WT was found despite lack of significantly different values for traits such as total VLA or larger xylem conduit sizes and/or numbers, which we had expected to correlate positively with K_{leaf} (McKown *et al.* 2010; Sack & Scoffoni 2013). However, we found strong correlation across all genotypes between K_{leaf} and the anatomical index of conductance of water across the BS (Fig. 5d; Supporting Information Table S3), which supports the expectation that hydraulic function is highly dependent upon BS conductance. The BS has been suggested as a bottleneck to hydraulic transport in the leaf based upon studies of turgor pressure and aquaporin activity in *A. thaliana* (Ache *et al.* 2010; Prado *et al.* 2013). Indeed, our findings support the proposal by Griffiths *et al.* (2013) that the importance of BS anatomy for overall hydraulic conductance of water to the mesophyll would be equal to or stronger than that of VLA.

We found that K_{leaf} was associated with the length and structure of the outside xylem path through BS cells (BS radial diameter, number of BS cells and the relationship to minor VLA; K_{bs}'; Figs 4g,h & 5a–d), as expected if significant resistance is found in the apoplastic or symplastic flow through the BS (Cochard *et al.* 2007). The flow across membranes within the vein and across the BS would also be expected to play a role, as aquaporin-mediated water transport strongly influences K_{leaf} (Postaire *et al.* 2010). Recently, Sade *et al.* (2014) found that K_{leaf} was significantly reduced in mutants with BS aquaporin expression silenced as compared to the WT. Further, aquaporins are known to play a general role in the regulation of transmembrane water transport

during plant growth and stress responses (Maurel 1997), and in particular have been found to decrease BS permeability during drought (Shatil-Cohen *et al*. 2011). In addition, the degree of suberization of the BS walls may have an effect. Future work is needed to further clarify the influence of BS anatomy on hydraulic flow pathways in *A. thaliana* and across diverse species. Indeed, our findings suggest that anatomy, along with permeability and aquaporin activation/expression, can overshadow the differences in vein length or numbers of xylem conduits in determining K_{leaf} differences among genotypes of a species. Such a finding is consistent with and provides a potential explanation for the findings of recent studies of genotypes of *Coffea arabica* (Nardini *et al*. 2014) and cultivars of *Oryza* (Xiong *et al*. 2014), which did not find a positive correlation of K_{leaf} with VLA.

Importance of vein traits and biochemistry in determining differences in hydraulic performance

Our study supported the influence of vein traits, particularly the BS, on K_{leaf}. We generally expect traits that vary most to have the greatest influence on K_{leaf} against a background of other traits that remain similar, and this depends upon the set of plants examined (Sack & Scoffoni 2013). In *A. thaliana*, overall leaf morphology was relatively similar across the tested genotypes, yielding different results than those across diverse species. For example, in most angiosperm species, minor veins account for >85% of the total VLA (Sack & Scoffoni 2012; Sack *et al*. 2012), but in *A. thaliana*, the ratio of minor:total VLA is much lower, and major veins are more important (in this study minor:total VLA ranged from 0.51 to 0.59). Thus, while across diverse species VLA is often a strong driver of K_{leaf} (Sack & Frole 2006; Brodribb *et al*. 2007), among genotypes, the anatomical differences in BS traits may be a stronger influence. A general importance of the BS in determining K_{leaf} differences within a species requires confirmation, especially for species with a larger proportion of high-order veins.

Further research is needed to uncover the relative roles of vein and outside xylem traits in determining K_{leaf} across a broader range of *A. thaliana* genotypes. Our work is novel in showing strong variation in K_{leaf} and a first support for the hypothesis (3) of vein and anatomical traits in influencing hydraulic conductance across leaves for a mutant system. Our study demonstrates that structural variation in these genotypes scales up to functional consequences for the hydraulic system. Future studies can therefore clarify, on the one hand, the genetic basis for these traits, including aquaporin genes and expression, and on the other hand, the consequences for plant performance under different resource supplies. Such detailed knowledge for a model system will confirm and extend a unified understanding of leaf venation and its influence on plant growth and adaptation. Further work on the hydraulic properties of *A. thaliana* can clarify their role in the dynamics of growth. For example, K_{leaf} is sensitive to external factors such as environmental conditions, canopy position and time of day (Õunapuu & Sellin 2013), and the substantial variation in K_{leaf} between WT and mutants may be echoed in whole leaf performance based upon evidence of the positive relationship between K_{leaf}, photosynthesis and growth (Sack & Frole 2006; Brodribb *et al*. 2007; Maherali *et al*. 2008). Thus, future studies are needed to determine to what degree variation in hydraulic traits and leaf anatomy, and in particular, BS traits, might scale up to influencing gas exchange and growth across *A. thaliana* genotypes.

ACKNOWLEDGMENTS

We thank F. Carland and T. Nelson for providing seeds and advice for mutant selection and plant cultivation; W. Deng, G. John, C. Scoffoni, M. Bartlett, R. Mendez-Alonzo, A. Rowat, M. Ng and J. Smith for logistical assistance; and K. F. Hein Foundation for travel funds to F. Bongers. This work was supported by NSF grant IOS-1147292 and NSF GRFP grant DGE-1144087.

REFERENCES

Aasamaa K., Sober A. & Rahi M. (2001) Leaf anatomical characteristics associated with shoot hydraulic conductance, stomatal conductance and stomatal sensitivity to changes of leaf water status in temperate deciduous trees. *Australian Journal of Plant Physiology* **28,** 765–774.

Aasamaa K., Niinemets U. & Sober A. (2005) Leaf hydraulic conductance in relation to anatomical and functional traits during *Populus tremula* leaf ontogeny. *Tree Physiology* **25,** 1409–1418.

Ache P., Bauer H., Kollist H., Al-Rasheid K.A.S., Lautner S., Hartung W. & Hedrich R. (2010) Stomatal action directly feeds back on leaf turgor: new insights into the regulation of the plant water status from non-invasive pressure probe measurements. *The Plant Journal* **62,** 1072–1082.

Aloni R. (2001) Foliar and axial aspects of vascular differentiation: hypotheses and evidence. *Journal of Plant Growth Regulation* **20,** 22–34.

Ball R.A. & Oosterhuis D.M. (2005) Measurement of root and leaf osmotic potential using the vapor-pressure osmometer. *Environmental and Experimental Botany* **53,** 77–84.

Barigah T.S., Aussenac G., Baraloto C., Bonal D., Cochard H., Granier A., . . . Tyree M.T. (2013) The water relations of two tropical rainforest species (*Virola surinamensis* and *Eperua falcata*): is Virola unusual as previously reported? *Journal of Plant Hydraulics* **1,** e0002.

Benjamini Y. & Hochberg Y. (1995) Controlling the false discovery rate: a practical and powerful approach to multiple testing. *Journal of the Royal Statistical Society: Series B (Methodological)* **57,** 289–300.

Berlyn G.P. & Miksche J.P. (1976) *Botanical Microtechnique and Cytochemistry*. Iowa State University Press, Ames, IA.

Blackman C.J., Brodribb T.J. & Jordan G.J. (2009) Leaf hydraulics and drought stress: response, recovery and survivorship in four woody temperate plant species. *Plant, Cell & Environment* **32,** 1584–1595.

Boyce C.K., Brodribb T.J., Field T.S. & Zwieniecki M.A. (2008) Angiosperm leaf vein evolution was physiologically and environmentally transformative. *Proceedings of the Royal Society B* **276,** 1771–1776.

Brodribb T.J., Field T.S. & Jordan G.J. (2007) Leaf maximum photosynthetic rate and venation are linked by hydraulics. *Plant Physiology* **144,** 1890–1898.

Brodribb T.J., Feild T.S. & Sack L. (2010) Viewing leaf structure and evolution from a hydraulic perspective. *Functional Plant Biology* **37,** 488–498.

Buckley T.N. (2014) The contributions of apoplastic, symplastic and gas phase pathways for water transport outside the bundle sheath in leaves. *Plant, Cell & Environment* **38,** 7–22.

Caldeira C.F., Jeanguenin L., Chaumont F. & Tardieu F. (2014) Circadian rhythms of hydraulic conductance and growth are enhanced by drought and improve plant performance. *Nature Communications* **5,** 5365.

Candela H., Martinez-Laborda A. & Micol J.L. (1999) Venation pattern formation in *Arabidopsis thaliana* vegetative leaves. *Developmental Biology* **205,** 205–216.

Carland F.M. & Nelson T. (2004) Cotyledon vascular pattern2-mediated inositol (1, 4, 5) triphosphate signal transduction is essential for closed venation patterns of *Arabidopsis foliar* organs. *The Plant Cell* **16,** 1263–1275.

Carland F.M., Berg B.L., FitzGerald J.N., Jinamornphongs S., Nelson T. & Keith B. (1999) Genetic regulation of vascular tissue patterning in *Arabidopsis*. *The Plant Cell* **11,** 2123–2137.

Carland F.M., Fujioka S., Takatsuto S., Yoshida S. & Nelson T. (2002) The identification of CVP1 reveals a role for sterols in vascular patterning. *The Plant Cell* **14,** 2045–2058.

Chatelet D.S., Clement W.L., Sack L., Donoghue M.J. & Edwards E.J. (2013) The evolution of photosynthetic anatomy in Viburnum (Adoxaceae). *International Journal of Plant Sciences* **174,** 1277–1291.

Choat B. (2011) Hydraulic conductance and conductivity. PrometheusWiki. http://Prometheuswiki.publish.csiro.au/tiki-index.php?page=Hydraulic+conductance+and+conductivity.

Clay N.K. & Nelson T. (2005) *Arabidopsis* thickvein mutation affects vein thickness and organ vascularization, and resides in a provascular cell-specific spermine synthase involved in vein definition and in polar auxin transport. *Plant Physiology* **138,** 767–777.

Cochard H., Nardini A. & Coll L. (2004) Hydraulic architecture of leaf blades: where is the main resistance? *Plant, Cell & Environment* **27,** 1257–1267.

Cochard H., Venisse J.S., Barigah T.S., Brunel N., Herbette S., Guilliot A., . . . Sakr S. (2007) Putative role of aquaporins in variable hydraulic conductance of leaves in response to light. *Plant Physiology* **143,** 122–133.

Dettmann S., Perez C.A. & Thomas F.M. (2013) Xylem anatomy and calculated hydraulic conductance of four *Nothofagus* species with contrasting distribution in South-Central Chile. *Trees* **27,** 685–696.

Dow G.J., Berry J.A. & Bergmann D.C. (2014) The physiological importance of developmental mechanisms that enforce proper stomatal spacing in *Arabidopsis thaliana*. *New Phytologist* **201,** 1205–1217.

Ellis B., Daly D.C., Hickey L.J., Mitchell J.D., Johnson K.R., Wilf P. & Wing S.L. (2009) *Manual of Leaf Architecture*. Cornell University Press, Ithaca, NY.

Griffiths H., Weller G., Toy L.F.M. & Dennis R.J. (2013) You're so vein: bundle sheath physiology, phylogeny and evolution in C_3 and C_4 plants. *Plant, Cell & Environment* **36,** 249–261.

Kang J. & Dengler N. (2004) Vein pattern development in adult leaves of *Arabidopsis thaliana*. *International Journal of Plant Sciences* **165,** 231–242.

Krober W., Heklau H. & Bruelheidi H. (2014) Leaf morphology of 40 evergreen and deciduous broadleaved subtropical tree species and relationships to functional ecophysiological traits. *Plant Biology* **17,** 373–383.

Lawson S.S., Pijut P.M. & Michler C.H. (2014) Comparison of *Arabidopsis* stomatal density mutants indicates variation in water stress responses and potential epistatic effects. *Journal of Plant Biology* **57,** 162–173.

Levin M., Lemcoff J.H., Cohen S. & Kapulnik Y. (2007) Low air humidity increases leaf-specific hydraulic conductance of *Arabidopsis thaliana* (L.) Heynh (Brassicaceae). *Journal of Experimental Botany* **58,** 3711–3718.

Lewis A.M. & Boose E.R. (1995) Estimating flow rates through xylem conduits. *American Journal of Botany* **82,** 1112–1116.

McKown A.D., Cochard H. & Sack L. (2010) Decoding leaf hydraulics with a spatially explicit model: principles of venation architecture and implications for its evolution. *American Naturalist* **175,** 447–460.

Maherali H., Sherrard M.E., Clifford M.H. & Latta R.G. (2008) Leaf hydraulic conductivity and photosynthesis are genetically correlated in an annual grass. *New Phytologist* **180,** 240–247.

Maurel C. (1997) Aquaporins and water permeability of plant membranes. *Annual Review in Plant Physiology and Plant Molecular Biology* **48,** 399–429.

Nardini A., Õunapuu-Pikas E. & Savi T. (2014) When smaller is better: leaf hydraulic conductance and drought vulnerability correlate to leaf size and venation density across four *Coffea arabica* genotypes. *Functional Plant Biology* **41,** 972–982.

Nobel P.S., Zaragoza L.J. & Smith W.K. (1975) Relation between mesophyll surface area, photosynthetic rate, and illumination level during development for leaves of *Plectranthus parviflorus* Henckel. *Plant Physiology* **55,** 1067–1070.

Noblin X., Mahadevan L., Coomaraswamy I.A., Weitz D.A., Holbrook N.M. & Zwieniecki M.A. (2008) Optimalvein density in artificial and real leaves. *Proceedings of the National Academy of Sciences of the United States of America* **105,** 9140–9144.

Oguchi R., Hikosaka K. & Hirose T. (2005) Leaf anatomy as a constraint for photosynthetic acclimation: differential responses in leaf anatomy to increasing growth irradiance among three deciduous trees. *Plant, Cell & Environment* **28,** 916–927.

Oosterhuis D.M., Savage M.J. & Walker S. (1983) Field use of in situ leaf psychrometers for monitoring water potential of a soybean crop. *Field Crops Research* **7,** 237–248.

Õunapuu E. & Sellin A. (2013) Daily dynamics of leaf and soil-to-branch hydraulic conductance in silver birch (*Betula pendula*) measured in situ. *Plant Physiology and Biochemistry* **68,** 104–110.

Petricka J.J., Clay N.K. & Nelson T.M. (2008) Vein patterning screens and the defectively organized tributaries mutants in *Arabidopsis thaliana*. *The Plant Journal* **56,** 251–263.

Postaire O., Tournaire-Roux C., Grondin A., Boursiac Y., Morillon R., Schaffner A.R. & Maurel C. (2010) A PIP1 aquaporin contributes to hydrostatic pressure-induced water transport in both the root and rosette of *Arabidopsis*. *Plant Physiology* **152,** 1418–1430.

Prado K., Boursiac Y., Tournaire-Roux C., Monneuse J.M., Postaire O., Da Ines O., . . . Maurel C. (2013) Regulation of *Arabidopsis* leaf hydraulics involves light-dependent phosphorylation of aquaporins in veins. *The Plant Cell* **25,** 1029–1039.

Robles P., Fleury D., Candela H., Cnops G., Alsonso-Peral M.M., Anami S., . . . Micol J.L. (2010) The RON1/FRY1/SAL1 gene is required for leaf morphogenesis and venation patterning in *Arabidopsis*. *Plant Physiology* **152,** 1357–1372.

Rockwell F.E., Holbrook N.M. & Stroock A.D. (2014) The competition between liquid and vapor transport in transpiring leaves. *Plant Physiology* **164,** 1741–1758.

Sachs T. (1975) The control of differentiation of vascular networks. *Annals of Botany* **39,** 197–204.

Sack L. & Frole K. (2006) Leaf structural diversity is related to hydraulic capacity in tropical rainforest trees. *Ecology* **87,** 483–491.

Sack L. & Holbrook N.M. (2006) Leaf hydraulics. *Annual Review of Plant Biology* **57,** 361–381.

Sack L. & Scoffoni C. (2012) Measurement of leaf hydraulic conductance and stomatal conductance and their responses to irradiance and dehydration using the evaporative flux method (EFM). *Journal of Visualized Experiments* **31,** pii: 4179. http://www.jove.com/video/4179/measurement-leaf-hydraulic-conductance-stomatal-conductance-their.

Sack L. & Scoffoni C. (2013) Leaf venation: structure, function, development, evolution, ecology and applications in the past, present and future. *New Phytologist* **198,** 983–1000.

Sack L., Melcher P.J., Zwieniecki M.A. & Holbrook N.M. (2002) The hydraulic conductance of the angiosperm leaf lamina: a comparison of three measurement methods. *Journal of Experimental Botany* **53,** 2177–2184.

Sack L., Scoffoni C., McKown A.D., Frole K., Rawls M., Havran J.C., . . . Tran T. (2012) Developmentally based scaling of leaf venation architecture explains global ecological patterns. *Nature Communications* **3,** 837.

Sack L., Caringella M., Scoffoni C., Mason C., Rawls M., Markesteijn L. & Poorter L. (2014) Leaf vein length per unit area is not intrinsically dependent on image magnification: avoiding measurement artifacts for accuracy and precision. *Plant Physiology* **166,** 829–838.

Sade N., Shatil-Cohen A., Attia Z., Maurel C., Boursiac Y., Kelly G., . . . Moshelion M. (2014) The role of plasma membrane aquaporins in regulating the bundle sheath-mesophyll continuum and leaf hydraulics. *Plant Physiology* **166,** 1609–1620.

Scarpella E., Francis P. & Berleth T. (2004) Stage-specific markers define early steps of procambium development in *Arabidopsis* leaves and correlate termination of vein formation with mesophyll differentiation. *Development (Cambridge, England)* **131,** 3445–3455.

Scoffoni C., McKown A.D., Rawls M. & Sack L. (2012) Dynamics of leaf hydraulic conductance with water status: quantification and analysis of species differences under steady state. *Journal of Experimental Botany* **63,** 643–658.

Shatil-Cohen A., Attia Z. & Moshelion M. (2011) Bundle-sheath cell regulation of xylem-mesophyll water transport via aquaporins under drought stress: a target of xylem-borne ABA? *The Plant Journal* **67,** 72–80.

Sieburth L.E. & Deyholos M.K. (2006) Vascular development: the long and winding road. *Current Opinion in Plant Biology* **9,** 48–54.

Tixier A., Cochard H., Badel E., Dusotoit-Coucaud A., Jansen S. & Herbette S. (2013) *Arabidopsis thaliana* as a model species for xylem hydraulics: does size matter? *Journal of Experimental Botany* **64,** 2295–2305.

Tosens T., Niinemets U., Westoby M. & Wright I.J. (2012) Anatomical basis of variation in mesophyll resistance in eastern Australian sclerophylls: news of a long and winding path. *Journal of Experimental Botany* **63,** 5105–5119.

Turner S. & Sieburth L.E. (2003) Vascular patterning. In *The Arabidopsis Book* Vol. **2,** p. e0073. American Society of Plant Biologists. doi: 10.1199/tab.0073.

Tyree M.T. & Zimmermann M.H. (2002) *Xylem Structure and the Ascent of Sap*. Springer, Berlin.

Wagner R., Aigner H., Pruzinska A., Jankanpaa H.J., Jansson S. & Funk C. (2011) Fitness analyses of *Arabidopsis thaliana* mutants depleted of FtsH metalloproteases and characterization of three FtsH6 deletion mutants exposed to high light stress, senescence and chilling. *New Phytologist* **191,** 449–458.

Weast R.C. (ed.) (1974) *Handbook of Chemistry and Physics*. 54th edn, CRC Press, Cleveland, OH.

Wylie R. (1939) Relations between tissue organization and vein distribution in dicotyledon leaves. *American Journal of Botany* **26,** 219–225.

Xiong D., Yu T., Zhang T., Li Y., Peng S. & Huang J. (2014) Leaf hydraulic conductance is coordinated with leaf morpho-anatomical traits and nitrogen status in the genus *Oryza*. *Journal of Experimental Botany* **66,** 741–748.

Yang S.D. & Tyree M.T. (1993) Hydraulic resistance in *Acer saccharum* shoots and its influence on leaf water potential and transpiration. *Tree Physiology* **12,** 231–242.

Received 14 November 2014; received in revised form 28 May 2015; accepted for publication30 May 2015

SUPPORTING INFORMATION

Additional Supporting Information may be found in the online version of this article at the publisher's web-site:

Table S1. Mean and SE for measured traits.

Table S2. Comparison of minor VLA, total VLA and FEV/A means ± SE using method 1 and method 2 (corrected for VPAA1°, 2°, 3°).

Table S3. Correlation matrix for the 5 genotypes (Col-O, dot3-111, dot3-134, cvp1-3, cvp2-1) correlations for untransformed and log-transformed data shown with significance ($*P < 0.05$, $**P < 0.01$, $***P < 0.001$).

Table S4. Mean ± SE K_{leaf} and corresponding E (transpiration) and final Ψ_{leaf} (leaf water potential) values measured for the WT and four mutants.

Table S5. ANOVA results comparing among all 5 genotypes, and among 4 mutant genotypes nested within class/type (*dot* mutants are parallel class and *cvp* mutants are open network class).